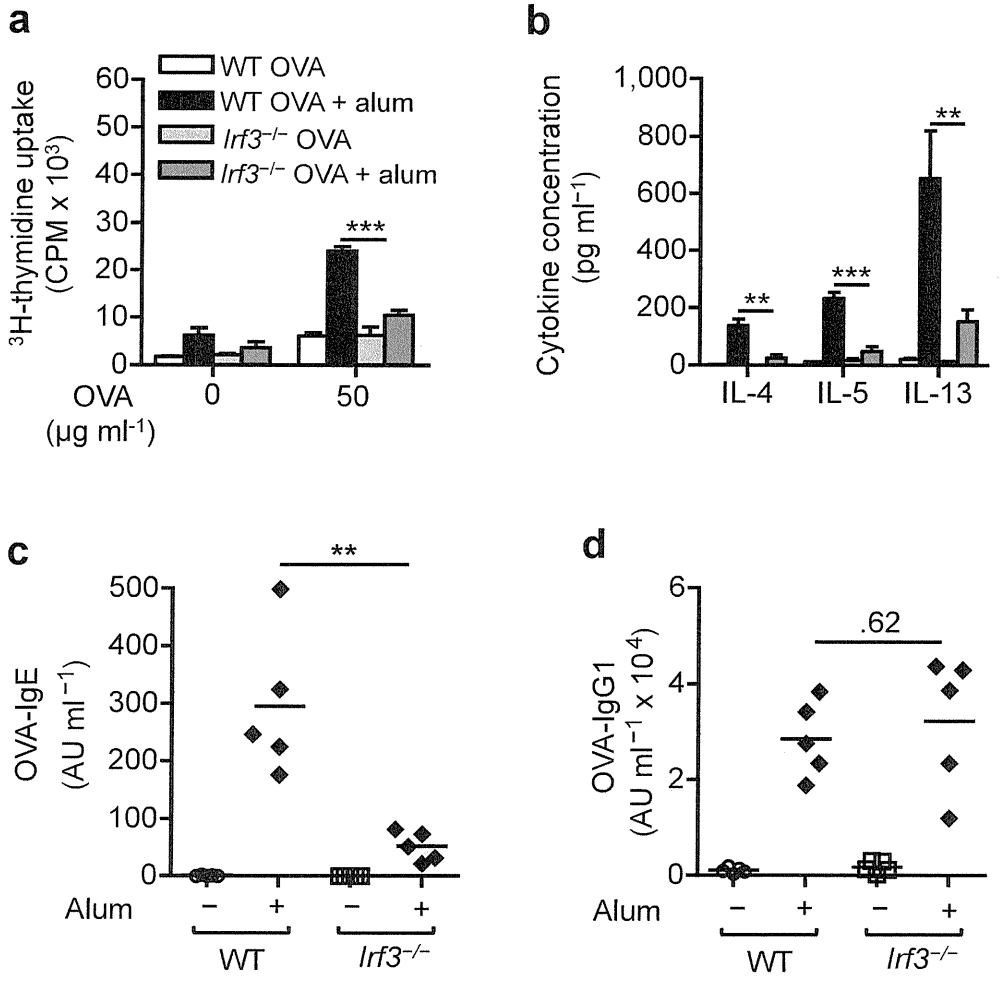

Supplementary Figure 9 Irf3 is essential for the boosting of 'canonical' Th2 cell differentiation and IgE responses in an alum-immunization-based asthma model. We challenged OVA- and OVA and alum-sensitized WT and *Irf3*$^{-/-}$ mice with aerosolized OVA and analyzed for type 2 T cell and humoral responses. (**a**) BLN cell proliferation in response to 3 days *in vitro* OVA stimulation assessed by the measurement of ^{3}H-thymidine uptake. (**b**) ELISA measurement of IL-4, IL-5 and IL-13 concentrations in culture supernatants of OVA-stimulated BLN cells. Serum OVA-specific IgE (**c**) and IgG1 (**d**) titers. *n*=5. Data are representative of one of three independent experiments. (CPM, counts per minute).

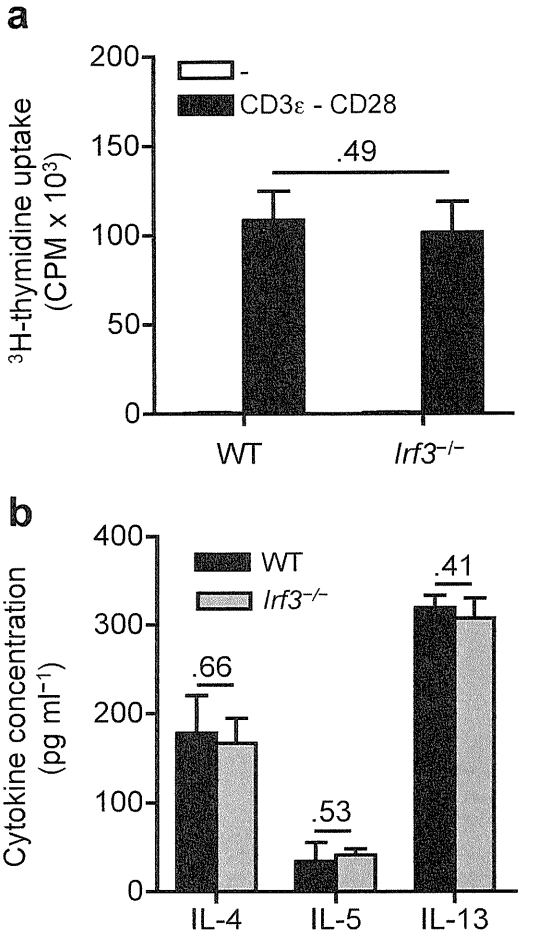

Supplementary Figure 10 WT and *Irf3*$^{-/-}$ T lymphocytes have similar potential for proliferation and Th2 cytokine secretion. (**a**) Proliferation assessed by measuring ^{3}H-thymidine incorporation during the last 16 hours of a 2-day culture of T cells (2 10^5 cells, >95% purity) purified from the BLNs of naïve WT and *Irf3*$^{-/-}$ mice and cultured with CD28-specific antibodies into plates coated with CD3-specific antibodies. We cultured controls in uncoated wells without CD28-specific antibodies. (**b**) ELISA measurement of IL-4, IL-5, IL-13 in the supernatant of the cells in a. *n*=5 . Data are representative of one of three independent experiments. (CPM, counts per minute)

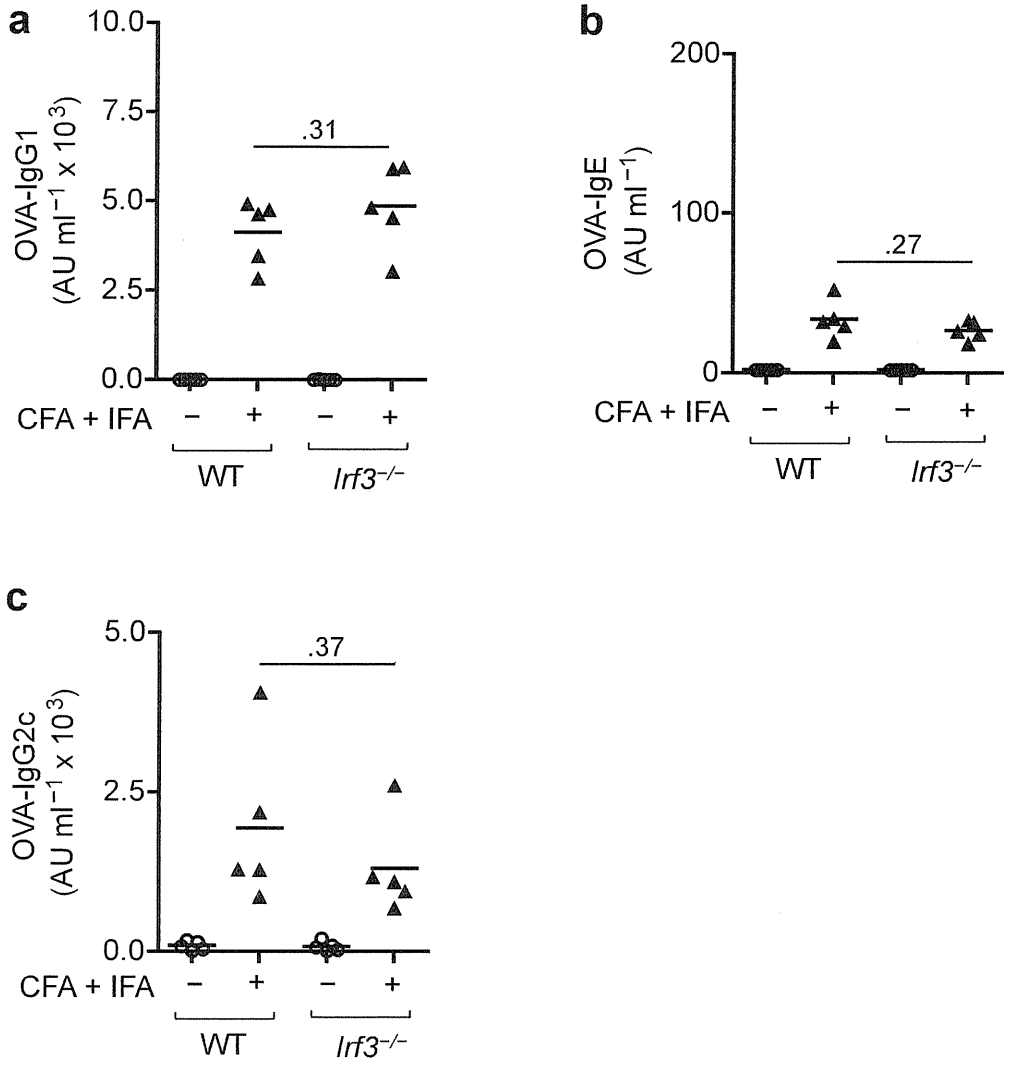

Supplementary Figure 11 *Irf3*$^{-/-}$ mice have normal immunization potential in response to Irf3-independent adjuvants. Serum OVA-specific IgG1 (**a**), IgE (**b**), and IgG2c (**c**) antibody titers measured on day 28 in WT and *Irf3*$^{-/-}$ mice immunized s.c. with OVA and CFA on day 0 and OVA and IFA on day 14, and boosted with OVA i.p. on day 21. *n*=5. Data are representative of one of two independent experiments. (AU, arbitrary unit).

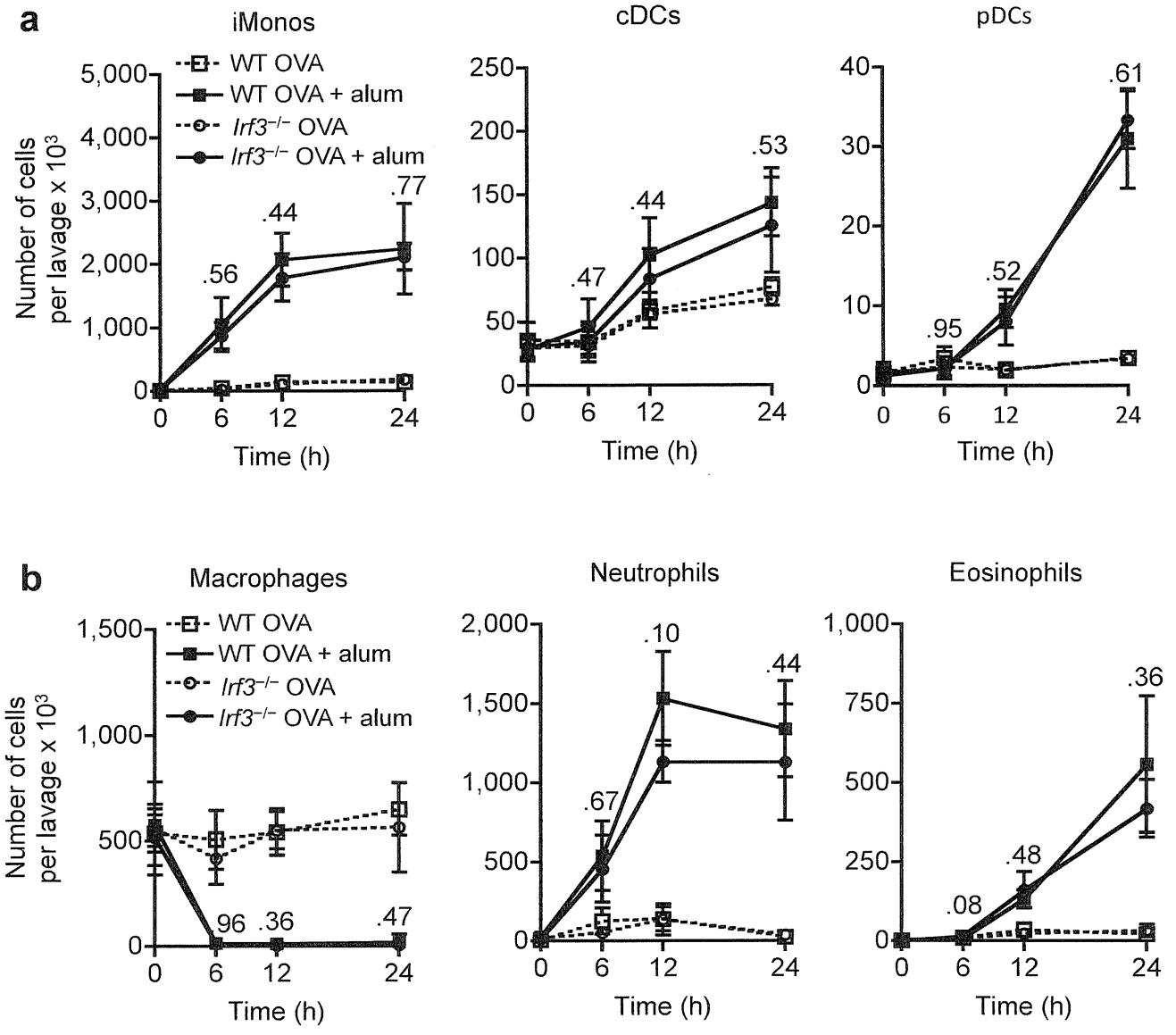

Supplementary Figure 12 Alum induces similar recruitment of innate immune cells in WT and *Irf3*$^{-/-}$ mice. Recruitment of innate immune cells through time in the peritoneal lavage fluid of WT and *Irf3*$^{-/-}$ mice treated i.p. with OVA or OVA and alum, assessed by flow cytometry. (**a**) We defined inflammatory monocytes (iMonos) as F4/80^{int} CD11b^{+} Ly6C^{+} Ly6G^{-} cells, conventional DCs (cDCs) as MHCII^{+} CD11c^{+} F4/80^{low} Ly6C^{-} cells, and plasmacytoid DCs (pDCs) as B220^{+} Ly6G^{+} CD11c^{int} F4/80^{low} cells. (**b**) We defined peritoneal macrophages as F4/80^{high} CD11b^{+} SSC^{high} cells, neutrophils as CD11b^{+} Ly6C^{+} Ly6G^{+} F4/80^{-} cells, and eosinophils as CD11b^{+} Ly6C^{int} Ly6G^{int} F4/80^{int} cells. *n*=5. Data are representative of one of four independent experiments.

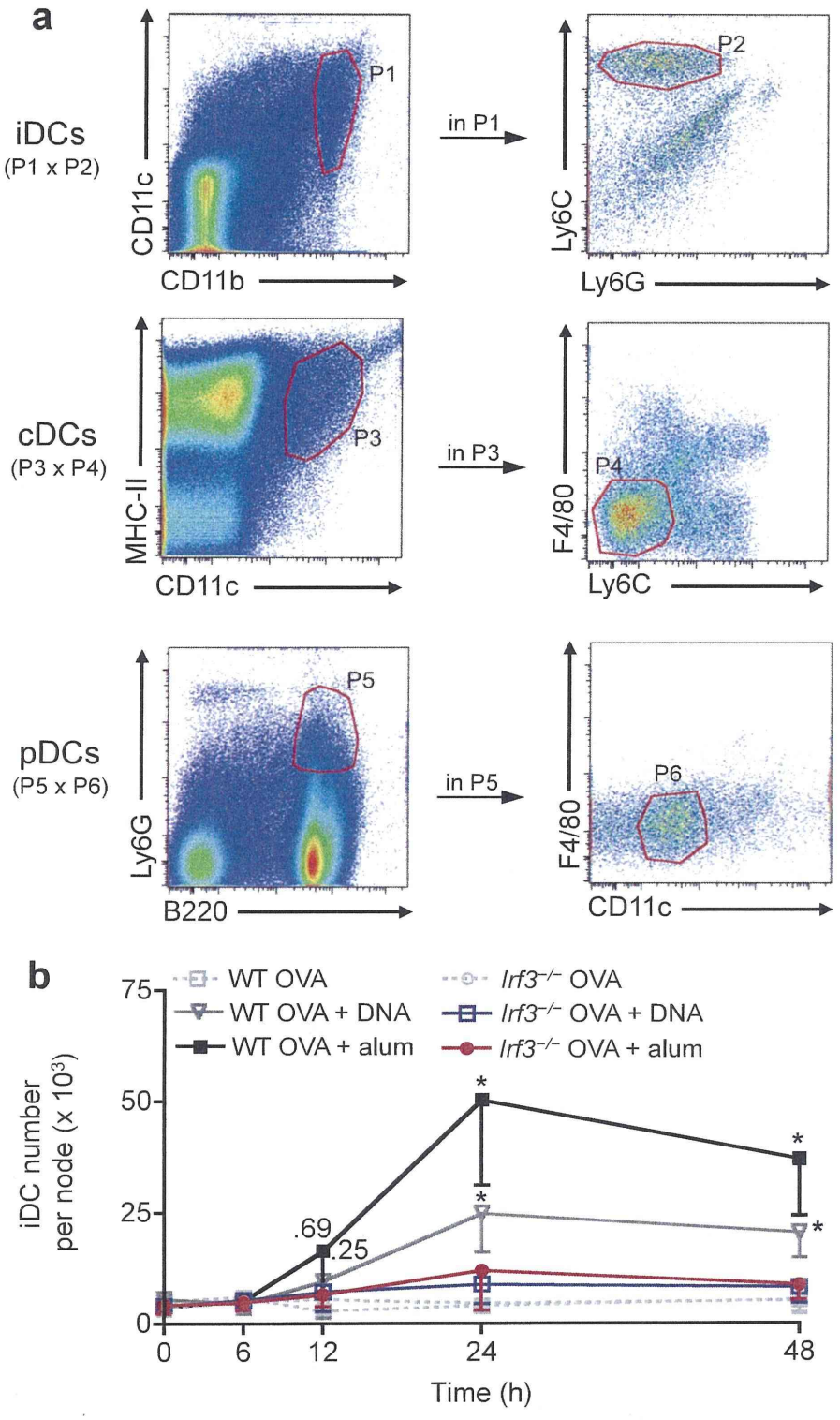

Supplementary Figure 13 Gating strategy and alum- and DNA-induced migration of iDCs. (**a**) Gating strategy for the identification of inflammatory dendritic cells (iDCs), conventional DCs (cDCs) and plasmacytoid DCs (pDCs) in the BLNs of mice by flow cytometry. We defined iDCs as CD11c$^{int/+}$ CD11b^{+} Ly6C^{+} Ly6G^{-} cells, cDCs as MHCII^{+} CD11c^{+} F4/80^{low} Ly6C^{-} cells and pDCs as B220^{+} Ly6G^{+} CD11c^{int} F4/80^{low} cells. (**b**) Comparison by flow cytometric analysis of the recruitment of iDCs to the BLNs of WT and Irf3$^{-/-}$ mice treated i.m. with OVA, OVA and DNA or OVA and alum. *n*=5. Data are representative of one of more than 4 (**a**) and one of two (**b**) independent experiments.

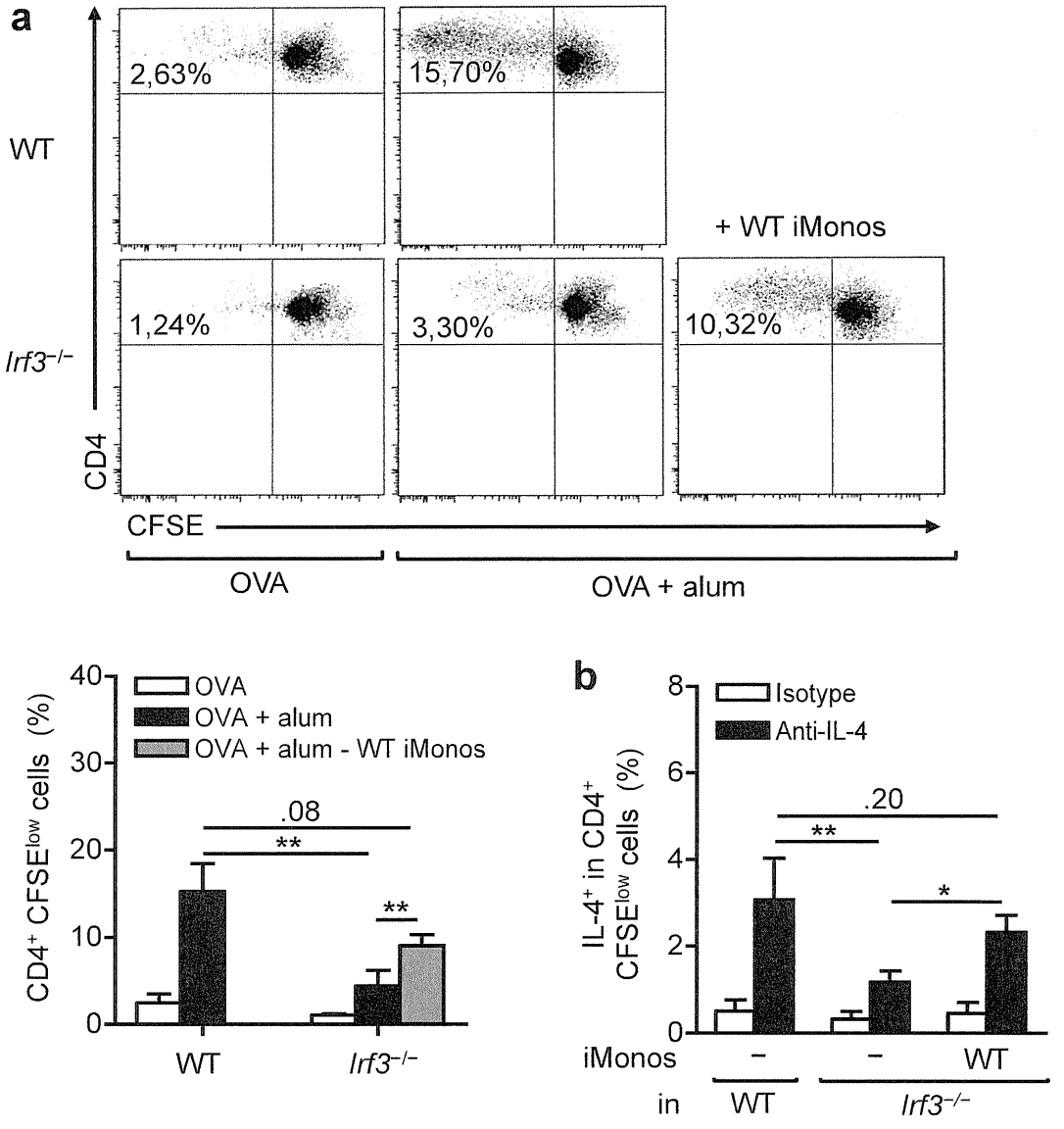

Supplementary Figure 14 Deficient inflammatory monocyte function is responsible for impaired type 2 responses in the lymph nodes draining alum injection sites in *Irf3*$^{-/-}$ mice. We treated *Irf3*$^{-/-}$ mice i.p. with OVA and alum and, 6 h later, injected them i.p. 2.10^6 iMonos isolated from the peritoneal cavity of OVA and alum-treated WT mice. Five days later, we labeled the BLN cells of recipient mice with CFSE and restimulated them *in vitro* with OVA for 5 days. (**a**) Proliferation of OVA-specific CD4$^+$ T cells estimated by measuring the percentage of CFSE^{low} CD4$^+$ T cells by flow cytometry (Inserts indicating the percentage of CFSE^{low} CD4$^+$ T cells). (**b**) Percentages of IL4$^+$ cells among CD4$^+$ CFSE^{low} cells assessed by intracellular staining and flow cytometry. We used BLN cells from WT and *Irf3*$^{-/-}$ mice that received PBS with OVA alone or OVA and alum as controls. *n*=4 . Data are representative of one of three independent experiments.

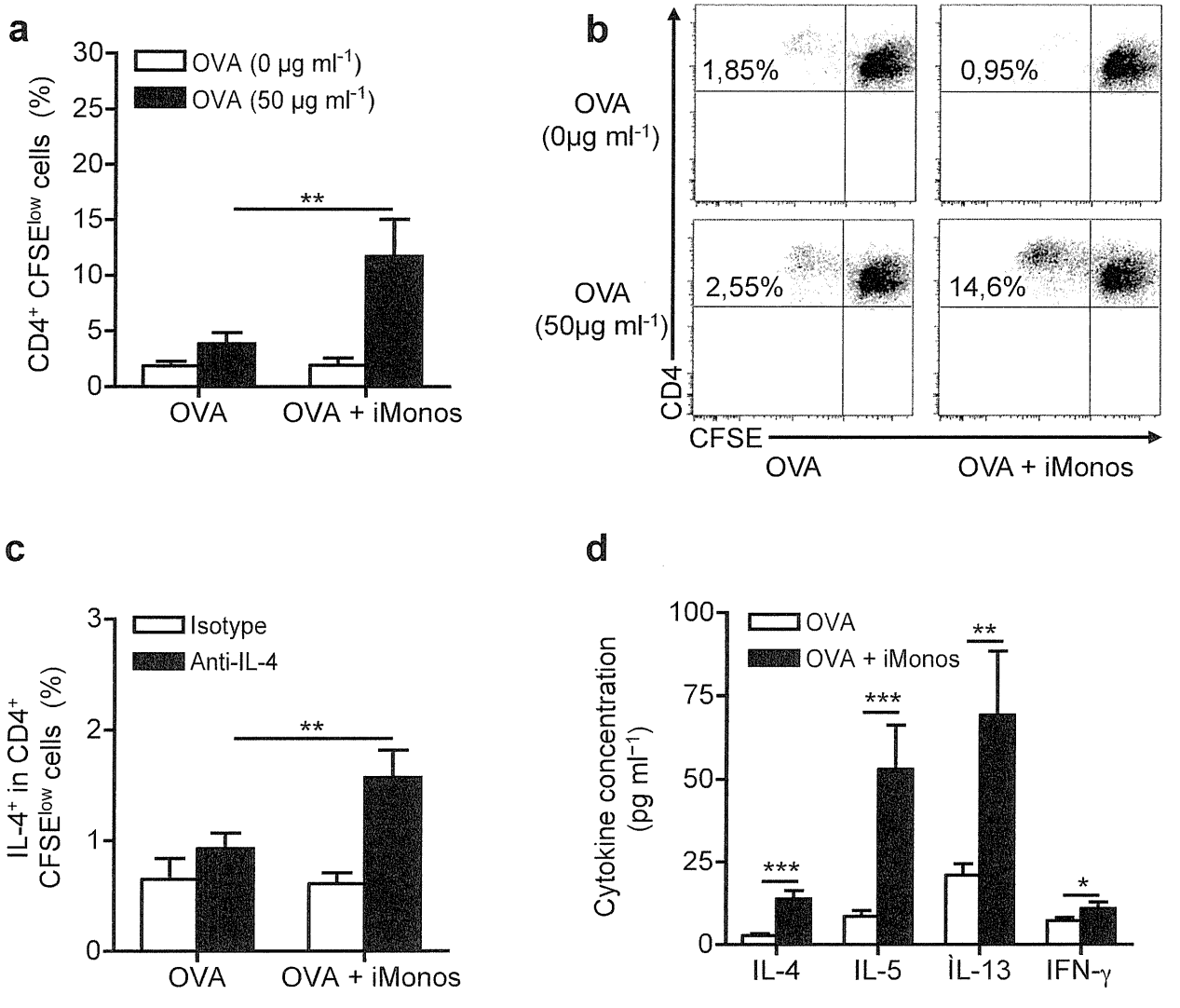

Supplementary Figure 15 Inflammatory monocytes are sufficient to induce type 2 responses in the lymph nodes draining alum injection sites. We gave WT mice i.p. 10 µg OVA alone or OVA with 2.10^6 iMonos isolated from the peritoneal cavity of OVA and alum-treated WT mice (OVA + iMonos). Five days later, we labeled the BLN cells of recipient mice with CFSE and restimulated them *in vitro* with or without OVA for 5 days. (**a**) Proliferation of OVA-specific $CD4^+$ T cells estimated by measuring the percentage of $CFSE^{low}$ $CD4^+$ T cells by flow cytometry. (**b**) Representative histograms of samples compared in (a), with inserts indicating the percentage of $CFSE^{low}$ $CD4^+$ T cells. (**c**) Percentages of $IL4^+$ cells among $CD4^+$ $CFSE^{low}$ cells assessed by intracellular staining and flow cytometry. (**d**) ELISA measurement of IL-4, IL-5, IL-13 and IFN-γ concentrations in the supernatant of the OVA-stimulated BLN cells. *n*=5 . Data are representative of one of two independent experiments. (iMonos, inflammatory monocytes).

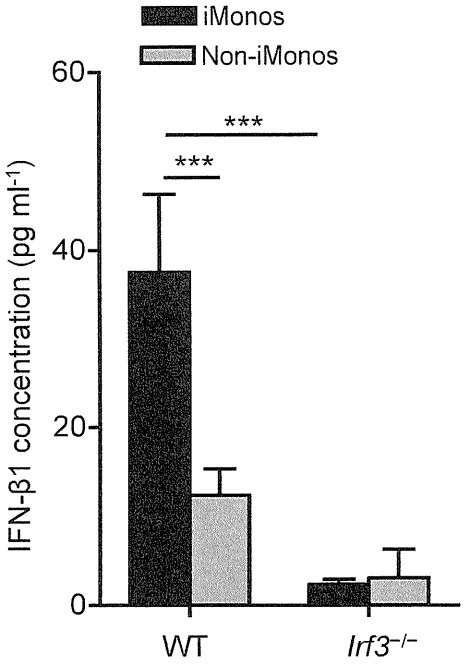

Supplementary Figure 16. Imonos are a major source of type I IFN production in alum-treated mice. IFN-β1 immunotrapping and ELISA detection in the supernatants of iMonos and negative fraction cells (non-iMonos) FACS-sorted from the peritoneal cavity of WT and *Irf3*$^{-/-}$ mice 18h after OVA and alum treatment. *n*=5. Data are representative of one of two independent experiments.

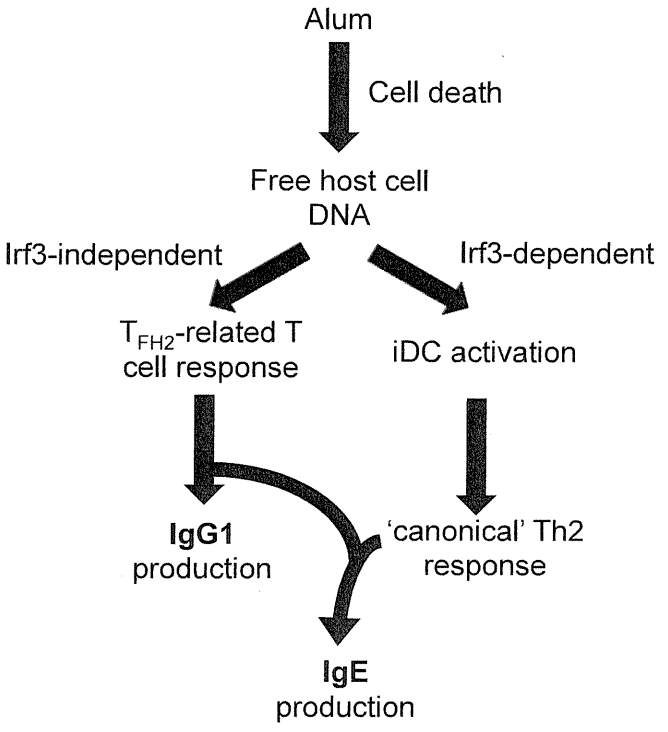

Supplementary Figure 17 Proposed model for the adjuvant effect of host cell DNA upon alum immunization.

Antibodies. Allophycocyanain- and phycoerythrin-conjugated F4/80 (BM8)-, allophycocyanain-conjugated Vα2 TCR (B20.1)-, allophycocyanain-eFluor780-conjugated CD11c (N418)-, eFluor450-conjugated CD11b (M1/70)-, fluorescein isothiocyanate-conjugated B220 (RA3-6B2)-, biotinylated CCR7 (4B12)-, CD86 (GL1)-, eFluor450-conjugated CD4 (RM4-5)-, CD3e (17A2)-specific antibodies and phycoerythrin-cyanin7-conjugated streptavidin were from eBioscience. Biotinylated anti–MHC class II (I-Ab; AF6-120.1)-, fluorescein isothiocyanate-conjugated-Ly6C (AL-21)-, allophycocyanin-conjugated-Ly6G (1A8)-, peridinin chlorphyll protein-cyanin5.5-conjugated-Ly6C (AL-21)-, allophycocyanain-conjugated IL-4- (11.B.11)-specific antibodies and phycoerythrin-conjugated streptavidin were from BD Biosciences. Fluorescein isothiocyanate–conjugated anti-CD40 (3/23) was from Serotec. Pacific-Blue-conjugated streptavidin was from Molecular Probes Invitrogen.

Lavage of injection sites and measurement of free double-stranded DNA concentrations and cell death rate. We performed lavages with 1 ml ice-cold Mg- and Ca-free PBS containing 0.6 mM EDTA. We removed cells and alum crystals from the lavage fluid of mice by 2 successive centrifugations at 1,000 g for 4 min at 4 °C. We measured double-stranded DNA in the acellular fraction of the lavage fluid using Quant-iT PicoGreen dsDNA reagent (Invitrogen) according to the manufacturer's protocol. We assessed cell death rate following alum treatment by staining with 5% (vol/vol) 7-AAD (e-Bioscience), followed by flow cytometric analysis.

Fluorescence microscopy. We isolated alum depots from injection sites 12 hours after treatment and incubated them for 10 minutes with 4',6-diamidino-2-phenylindole (DAPI). We then placed the depots in RMPI without phenol red, in a 35-mm glass bottom dish. We recorded images with an Olympus FV1000 confocal microscope equipped with a 60x oil objective and an incubation chamber to maintain the cells at 37 °C in a 5% CO_2 humidified atmosphere. We visualized DAPI fluorescence with a 405 nm excitation and a 415–480 nm emission window.

Peritoneal lavage transfer experiments. We performed peritoneal lavages 12 h after treatment with OVA and alum or OVA alone and removed cells and debris. We submitted peritoneal lavage fluids to DNase I digestion (Roche) for 5 h following the manufacturer's protocol. We mock-treated control peritoneal lavage fluids. We then gave recipient mice 400 μl of donor peritoneal lavage fluid or PBS mixed with 10 μg OVA i.p. We gave mice an i.p. boost of 20 μg OVA 10 d later. Mice were sacrificed for serum analysis one week later.

Immunizations with Freund's adjuvant. We injected mice on d 0 subcutaneously with 10 μg OVA alone or in conjunction with 400 μg CFA (Pierce Biochemicals). We collected serum on d 10. We injected mice subcutaneously on d 14 with 10 μg OVA alone or in conjunction with 400 μg IFA (Pierce Biochemicals). On d 21, we boosted mice i.p. with 20 μg alone and collected serum for analysis on d 28.

Restimulation of BLN cells. We cultured BLN cells (2 x 10^5 cells in a 96-well plate) in Click's medium (2.10^5 cells in 200 μl, in 96-well plates) supplemented with 0.5% (vol/vol) heat-inactivated C57 Bl/6 mouse serum (Harlan Netherland), 8 mM L-glutamin, 50 UI ml^{-1} G-penicillin and 50 μg ml^{-1} streptomycin, with or without OVA (OVA grade V, Sigma) (50 μg ml^{-1}). We collected culture supernatants for cytokine detection by ELISA. We measured cell proliferation as ^{3}H-thymidine incorporation during the last 16 h of a 4-d culture.

T-cell stimulation. We purified 2.10^5 cells T cells from BLNs using the Pan T cell Isolation Kit (Miltenyi Biotec) and assessed for purity by staining for CD3e followed by flow cytometry. We cultured cells with CD28-specific antibodies (5 mg ml^{-1}; 37.51, eBioscience) in RPMI supplemented with 10% (vol/vol) heat-inactivated FCS and additives into 96 well plates coated with CD3-specific antibodies (10 mg ml^{-1}; 145-2C11, eBioscience). We cultured controls in uncoated wells without CD28-specific antibodies. We measured cell proliferation was measured as ^{3}H-thymidine incorporation during the last 16 h of a 2-d culture.

CFSE labeling. We incubated splenic and lymph node cells from OT-II transgenic mice (5×10^7 cells/ml) with CFSE (5 μM in PBS) for 10 minutes at 37 °C. We washed cells in PBS containing 10% FCS and then twice in PBS and injected them in the caudal vein of mice.

Alum-induced asthma model. We challenged OVA- and OVA and alum-sensitized mice from d 21 to 25 with aerosolized OVA 1% (wt/vol) in PBS for 1 h per day. We performed broncho-alveolar lavages and cytology. Briefly, we catheterized the trachea and washed the lungs with 1 ml ice-cold Mg- and Ca-free PBS containing 0.6 mM EDTA. We assessed cell density in bronchoalveolar lavage fluid using a hemocytometer. We performed differential cell counts on cytospin preparations stained with Diff-Quick (Dade Behring). We fixed lungs in 10% formalin, paraffin-embedded them, and cut them in 5-mm sections. We estimated the extent of peribronchial inflammation by a score calculated by means of quantification of peribronchial inflammatory cell layers in lung sections stained with hematoxylin and eosin. We quantified mucus production as the percentage of periodic acid-Schiff-stained goblet cells per total epithelial cells in randomly selected bronchi. We randomly selected and analyzed seven sections per lung.

ELISA. We assayed culture supernatants for mouse IL-4, IL-5, IL-13 and IFN-γ by ELISA (Biosource/Invitrogen) according to the manufacturer's protocol. We assayed peritoneal lavage supernatants for mouse IFN-β1 and IL-1β by ELISA (PBL Interferon Source and Imtec Diagnostics NV, respectively) according to the manufacturer's protocol. We performed IFN-β1 immunotrapping by culturing FACS-sorted iMonos and negative fraction (4.10^6 cells/ml) overnight in capture antibody-coated 96 wells plates, followed by classical ELISA.

Cell viability. We assessed the viability of CFSE-labeled iMonos prior to adoptive transfer by means of DAPI staining and subsequent flow cytometric analysis. The survival of iMonos following labeling was high and comparable between WT and *Irf3*$^{-/-}$ cells (data not shown).

Cell transfer experiments. For the study of migration, we purified iMonos from the peritoneal lavage fluid of OVA and alum-treated mice by FACS 18 h post-treatment (>95% purity). We stained iMonos with CFSE at a concentration of 2 μM for 10 min at 37 °C, washed and tested their viability. We then injected 1.10^6 cells i.p. into recipient mice treated with OVA and alum 12 h before transfer, or into naïve WT mice. We gave control mice vehicle PBS. For the assessment of their effects on type 2 and humoral responses, we purified iMonos as above 6 h post-treatment, and injected 2.10^6 cells i.p. into recipient mice treated with OVA and alum 6 h before transfer.

Immunity
Article

Silica Crystals and Aluminum Salts Regulate the Production of Prostaglandin in Macrophages via NALP3 Inflammasome-Independent Mechanisms

Etsushi Kuroda,[1,*] Ken J. Ishii,[3,4] Satoshi Uematsu,[5] Keiichi Ohata,[6] Cevayir Coban,[6] Shizuo Akira,[5] Kosuke Aritake,[7] Yoshihiro Urade,[7] and Yasuo Morimoto[2]
[1]Department of Immunology and Parasitology
[2]Department of Occupational Pneumology
University of Occupational and Environmental Health, Japan, Kitakyushu, Fukuoka, 807-8555, Japan
[3]Laboratory of Adjuvant Innovation, National Institute of Biomedical Innovation, Ibaraki, Osaka, 567-0085, Japan
[4]Laboratory of Vaccine Science
[5]Laboratory of Host Defense
[6]Laboratory of Malaria Immunology WPI Immunology Frontier Research Center
Osaka University, Suita, Osaka, 565-0871, Japan
[7]Department of Molecular Behavioral Biology, Osaka Bioscience Institute, Suita, Osaka, 565-0874, Japan
*Correspondence: kuroetu@med.uoeh-u.ac.jp
DOI 10.1016/j.immuni.2011.03.019

SUMMARY

Particulates such as silica crystal (silica) and aluminum salts (alum) activate the inflammasome and induce the secretion of proinflammatory cytokines in macrophages. These particulates also induce the production of immunoglobulin E via a T helper 2 (Th2) cell-associated mechanism. However, the mechanism involved in the induction of type 2 immunity has not been elucidated. Here, we showed that silica and alum induced lipopolysaccharide-primed macrophages to produce the lipid mediator prostaglandin E_2 (PGE_2) and interleukin-1β (IL-1β). Macrophages deficient in the inflammasome components caspase 1, NALP3, and ASC revealed that PGE_2 production was independent of the NALP3 inflammasome. PGE_2 expression was markedly reduced in PGE synthase-deficient (*Ptges*$^{-/-}$) macrophages, and *Ptges*$^{-/-}$ mice displayed reduced antigen-specific serum IgE concentrations after immunization with alum or silica. Our results indicate that silica and alum regulate the production of PGE_2 and that the induction of PGE_2 by particulates controls the immune response in vivo.

INTRODUCTION

Some particulates and crystals can stimulate the innate immune system to induce inflammatory responses. In particular, aluminum salts (referred to as alum) and silica crystals can induce type 2 inflammatory responses, which are characterized by the accumulation of eosinophils at the site of injection and the elevation of antigen-specific serum IgE and IgG1 amounts in vivo (Aimanianda et al., 2009; Marrack et al., 2009; Kumar et al., 2009). However, the basis for the adjuvanticity of these particulates and the mechanisms by which they elicit type 2 immunity remain poorly understood.

In the innate immune system, macrophages and dendritic cells (DCs) function as the first line of defense against foreign antigens. These cells can recognize pathogen-associated molecular patterns (PAMPs) through pattern-recognition receptors (PPRs) and can induce inflammatory responses (Akira et al., 2006). NOD-like receptors (NLRs) are intracellular PRRs (Ye and Ting, 2008). Among the known NLRs, NALP3 (also known as NLRP3, Cryopyrin, CIAS1, or PYPAF1) is one of the best characterized. Upon activation, NALP3 forms a multiprotein complex with apoptosis-associated speck-like protein containing a caspase recruitment domain (ASC) and caspase-1. This complex, referred to as the NALP3 inflammasome, promotes the secretion of the proinflammatory cytokines interleukin-1β (IL-1β) and IL-18 by the action of caspase-1 (Franchi et al., 2009; Martinon et al., 2009; Schroder and Tschopp, 2010; Schroder et al., 2010). The activated NALP3 inflammasome contributes to antifungal host defense, antitumor immunity, and inflammation (Duewell et al., 2010; Ghiringhelli et al., 2009; Gross et al., 2009; Halle et al., 2008; Watanabe et al., 2008). In addition to being activated by PAMPs, the NALP3 inflammasome is also activated by ATP, various crystals (i.e., silica, asbestos and monosodium urate), and alum (Cassel et al., 2008; Dostert et al., 2008; Eisenbarth et al., 2008; Hornung et al., 2008). The NALP3 inflammasome has been shown to induce type 2 immune responses, and *Nalp3*$^{-/-}$ and *Asc*$^{-/-}$ mice display reduced type 2 immune responses to alum (Eisenbarth et al., 2008; Kool et al., 2008; Li et al., 2008). However, other reports have shown that the NALP3 inflammasome is dispensable for alum adjuvanticity (Franchi and Núñez, 2008; McKee et al., 2009). In addition, it has been reported that the NALP3 inflammasome is not required for antibody production in response to vaccination by the particulate adjuvant (Sharp et al., 2009). Thus, the role of the NALP3 inflammasome in the induction of type 2 immunity is still open to further investigation.

In addition to proinflammatory cytokines, lipid mediators such as prostaglandins (PGs) are also involved in the induction of

inflammatory responses (Narumiya, 2009). PGE_2, a well-characterized proinflammatory lipid mediator, is an arachidonic acid metabolite that is produced by various types of cells including antigen-presenting cells. Previous reports have shown that PGE_2 suppresses T helper 1 (Th1) cell-type responses by elevating intracellular cAMP concentrations in DCs, macrophages, and Th1 cells, thus inhibiting their ability to produce type 1 cytokines such as IL-12 and IFN-γ (Fabricius et al., 2010; Koga et al., 2009; Kuroda and Yamashita, 2003). In addition, PGE_2 can enhance IL-23 production by DCs and favors Th17 cell polarization and IL-17 production (Boniface et al., 2009; Yao et al., 2009). More recently, PGE_2 was shown to facilitate Th1 cell differentiation in the presence of IL-12 and high doses of the costimulatory CD28 antibody, via activation of the PI3-kinase pathway (Yao et al., 2009). Thus, PGE_2 has various functions in the regulation of immune responses. However, the involvement of PGE_2 in particulate-mediated adjuvanticity has not been investigated.

In this study, we showed that alum, silica, and ATP, which activate the NALP3 inflammasome, induced macrophages to produce IL-1β, IL-18 and PGE_2. Interestingly, PGE_2 production in macrophages was regulated by the spleen tyrosine kinase (Syk) and p38 MAP kinase pathway but did not depend on inflammasome activation. In addition, particulate-induced PGE_2 regulated antigen-specific serum IgE production in vivo. Our results suggest that the activation of the PGE_2 pathway by particulates may be an important signal for the induction of type 2 immune responses.

RESULTS

Silica, Alum, and ATP Induce PGE_2 Production in LPS-Primed Macrophages

Many reports have shown that alum, silica, and ATP stimulate macrophages to produce the caspase-1-dependent cytokines IL-1β and IL-18 by activating the NALP3 inflammasome (Cassel et al., 2008; Dostert et al., 2008; Eisenbarth et al., 2008; Hornung et al., 2008). These cytokines are thought to be important for regulation of immune responses. However, some studies have shown that caspase-1-dependent cytokines are dispensable for immune regulation (Franchi and Núñez, 2008; McKee et al., 2009; Sharp et al., 2009). Thus, we first ascertained whether inflammasome activators could induce the production of caspase-1-independent factor(s) in macrophages. To this end, we examined the production of several cytokines, chemokines and lipid mediators by macrophages in response to silica, alum and ATP. Silica, alum and ATP induced LPS-primed macrophages to produce IL-1β and IL-18, which is in agreement with previous reports (Cassel et al., 2008; Dostert et al., 2008; Eisenbarth et al., 2008; Hornung et al., 2008). These inflammasome activators also induced LPS-primed macrophages to produce PGE_2 (Figure 1A). A time-course analysis revealed that silica stimulation of LPS-primed macrophages for 2 hr was sufficient for detecting similar amounts of PGE_2 and IL-1β, in terms of pg/ml secreted (Figure 1B). In our experiments, we tested three different alum compounds: Imject alum (a mixture of aluminum hydroxide and magnesium hydroxide; Thermo Scientific), alhydrogel (aluminum hydroxide gel; Sigma-Aldrich) and LSL alum (aluminum hydroxide hydrate gel suspension; LSL). The experiments described in Figures 1A and 1B were performed with LSL alum as a stimulator. To test which alum compound was the most potent PGE_2 inducer in macrophages, we stimulated LPS-primed macrophages with the three different compounds. Each alum compound stimulated the production of PGE_2, but LSL alum (referred to hereafter as alum) induced the highest PGE_2 production in LPS-primed macrophages. Alhydrogel induced modest production of PGE_2 in LPS-primed macrophages, whereas Imject alum induced low amounts of PGE_2 (Figure S1A). It is important to note that LPS-primed macrophages did not produce any other well-characterized inflammatory cytokines or chemokines in response to silica (Figure S1B) or alum (data not shown).

Activated macrophages are known to produce PGD_2 (Mohri et al., 2003). Indeed, we found that LPS-primed macrophages produced PGD_2 in response to silica (Figure 1C). We also examined the effect of titanium dioxide (TiO_2), which does not cause severe inflammation on inhalational exposure and does not activate the NALP3 inflammasome (Cassel et al., 2008), on PGE_2 production by macrophages. As shown in Figure 1D, TiO_2 did not induce IL-1β or PGE_2 production in LPS-primed macrophages. Activation of the NALP3 inflammasome in DCs contributes to particulate-mediated adjuvanticity (Kool et al., 2008). Thus, we compared PGE_2 production by bone marrow (BM)-derived DCs and macrophages. BM-derived DCs produced IL-1β and PGE_2 in response to silica and alum, but the amounts of PGE_2 were markedly higher in macrophages than in DCs (Figure 1E). We have previously reported that macrophages from BALB/c mice produce higher amounts of PGE_2 than those from C57BL/6 mice (Kuroda et al., 2007; Kuroda and Yamashita, 2003). Macrophages from BALB/c mice produced ~2-fold greater amounts of IL-1β and PGE_2 in response to silica than macrophages from C57BL/6 mice (Figure 1F). Our observations are not restricted to mouse studies, given that human peripheral blood mononuclear cells (PBMCs) also produced PGE_2 and IL-1β in response to silica (Figure 1G). These results indicate that in addition to IL-1β and IL-18, macrophages also produce PG in response to silica, alum, and ATP.

Silica- and Alum-Induced PGE_2 Production Is Independent of the Activity of Caspase-1

IL-1β and IL-18 are known to induce PG production (Dinarello, 2002; Lee et al., 2004). However, simple exposure of LPS-primed macrophages to IL-1β and/or IL-18 did not induce the production of PGE_2 (Figure 2A). BM cells from WT and IL-1 receptor-deficient mice were cultured for 7 days with macrophage colony stimulating factor (M-CSF), and adherent macrophages were analyzed for silica- and alum-induced PGE_2 production. As shown in Figure 2B, WT and *Il1r1*$^{-/-}$ macrophages produced comparable amounts of PGE_2. In addition, treatment of silica- or alum-activated macrophages with a caspase-1 inhibitor significantly reduced their ability to produce IL-1β but did not affect their ability to produce PGE_2 (Figure 2C). Because silica and alum can induce cell death, we wanted to rule out the possibility that the enhanced production of PGE_2 in silica- and alum-activated macrophages was due to cell death. For this purpose, we measured cell death in silica- and alum-activated macrophages by quantifying the release of lactose dehydrogenase (LDH) into the culture media. Treatment of macrophages with a caspase-1 inhibitor reduced silica- and alum-induced

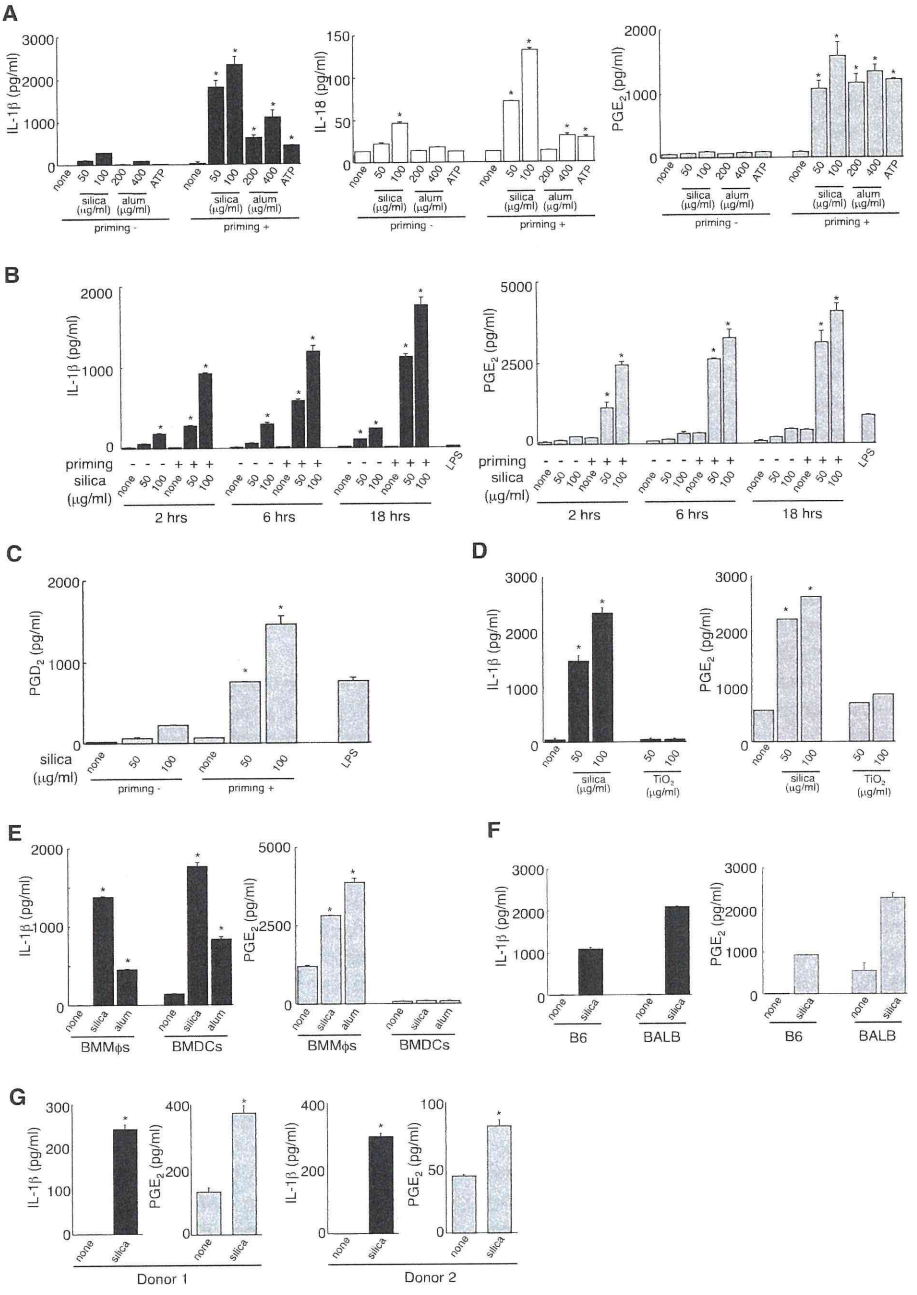

Figure 1. Inflammasome Activators Induce Macrophages to Produce PGE_2

(A) Peritoneal macrophages from BALB/c mice were primed for 3 hr with or without low-dose LPS (1 ng/ml) and then stimulated with silica, alum or ATP for 2 hr.

(B) Macrophages with or without LPS priming were stimulated with silica for 2, 6, or 18 hr. Macrophages stimulated with high-dose LPS (1 μg/ml) for 6 hr were used as controls.

(C) The culture supernatants of macrophages stimulated for 2 hr with silica were analyzed for PGD_2 production as indicated in (B).

(D) LPS-primed macrophages were stimulated with silica or TiO_2 for 2 hr.

(E) BM-derived macrophages and DCs were primed with LPS and then stimulated with 100 μg/ml silica or 400 μg/ml alum for 6 hr.

(F) Peritoneal macrophages from C57BL/6 (B6) and BALB/c (BALB) mice were primed with LPS and then stimulated with 100 μg/ml silica or 400 μg/ml alum for 2 hr.

(G) Human PBMCs were primed for 3 hr with LPS and then stimulated with silica for 3 hr. For all experiments, the amounts of IL-1β and PGE_2 in the culture supernatants were determined by ELISA. Data represent mean ± SE of three to five independent experiments (*$p < 0.01$).

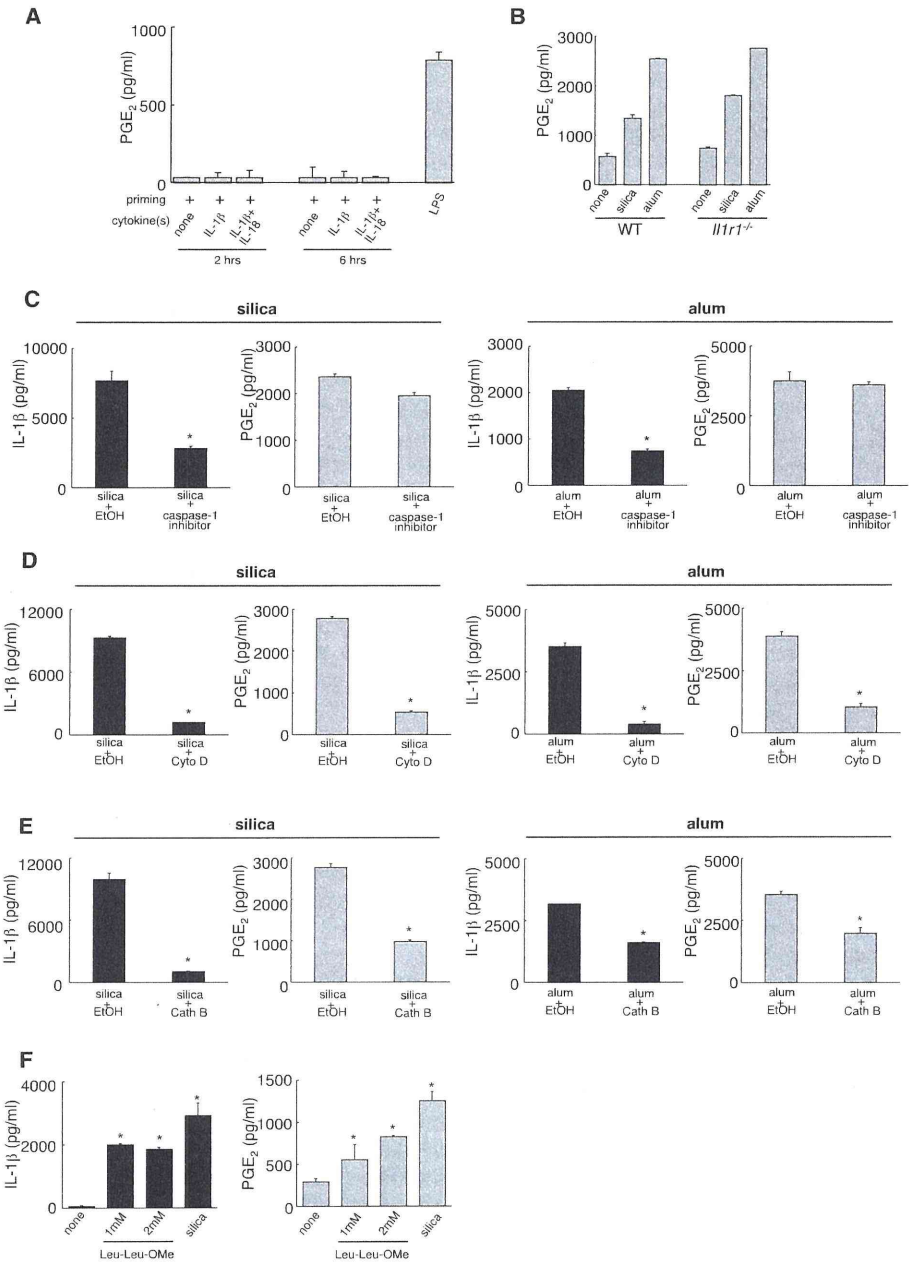

Figure 2. Silica- and Alum-Induced Lysosomal Damage Triggers PGE_2 Production in Macrophages via Caspase-1-Independent Mechanisms

(A) LPS-primed peritoneal macrophages were stimulated with IL-1β or IL-1β plus IL-18 for 2 or 6 hr. Macrophages stimulated with high-dose LPS were used as controls.

(B) M-CSF-derived BM macrophages from WT (C57BL/6) and *Il1r1*$^{-/-}$ mice were primed with low-dose LPS and then stimulated with 50 μg/ml silica or 200 μg/ml alum for 6 hr.

(C) LPS-primed macrophages were stimulated with 100 μg/ml silica or 400 μg/ml alum in the presence or absence of caspase-1 inhibitors for 2 hr.

(D and E) LPS-primed macrophages were stimulated with 100 μg/ml silica or 400 μg/ml alum in the presence or absence of cytochalasin D (D) or cathepsin B inhibitor (E) for 2 hr.

(F) LPS-primed macrophages were incubated with Leu-Leu-OMe for 2 hr. Data represent mean ± SE of three (A and C–E) or two (B and F) independent experiments (*$p < 0.01$).

cell death (Figure S2). This result was expected because caspase-1 is involved in promoting cell death. However, we have already shown that PGE_2 production in macrophages is independent of caspase-1 activity (Figure 2C and Figure S2). Therefore, these results indicate that caspase-1-dependent cytokine release and cell death are not responsible for silica- and alum-induced PGE_2 production in macrophages.

Silica and Alum Induce PGE_2 Production in Macrophages through Phagosomal Destabilization

Phagocytes engulf particulates such as silica or alum, which leads to lysosomal damage and rupture, followed by the release of lysosomal enzymes, such as cathepsin B, into the cytoplasm. Studies suggest that lysosomal damage can activate the NALP3 inflammasome and induce the production of IL-1β (Duewell et al., 2010; Hornung et al., 2008). To address whether the engulfment of particulates, lysosomal rupture, and release of lysosomal enzymes could induce PGE_2 production in macrophages, we cultured macrophages in the presence of cytochalasin D, which inhibits actin filament assembly and phagocytosis. Treatment of macrophages with cytochalasin D significantly reduced their ability to produce IL-1β and PGE_2 in response to silica and alum (Figure 2D).

The release of lysosomal enzymes such as cathepsin B is thought to trigger the activation of the NALP3 inflammasome. In addition, the cathepsin B inhibitor CA-074 has been shown to inhibit the NALP3 inflammasome (Duncan et al., 2009; Hornung et al., 2008; Sharp et al., 2009). We showed the production of IL-1β and PGE_2 by macrophages was partially inhibited by treating the cells with CA-074 (Figure 2E). Lysosomal damage has also been shown to trigger the activation of the NALP3 inflammasome. To investigate this process, we treated macrophages with leucyl-leucine methyl ester (Leu-Leu-OMe) to induce lysosomal damage (Hornung et al., 2008). Leu-Leu-OMe-treated macrophages produced large amounts of IL-1β (Figure 2F) as previously reported. Leu-Leu-OMe-treated macrophages also produced PGE_2. Altogether, these results suggest that, similar to the stimulatory effect of NALP3 inflammasome activation and IL-1β release, lysosomal damage and rupture triggers PGE_2 production in macrophages.

Silica- and Alum-Induced PGE_2 Production in Macrophages Is Independent of the NALP3 Inflammasome

We have shown that the NALP3 inflammasome activators silica, alum, and ATP induce LPS-primed macrophages to produce PGE_2. We have also demonstrated that PGE_2 production is independent of caspase-1 activity. To investigate whether the NALP3 inflammasome is involved in silica- and alum-induced PGE_2 production, we performed experiments similar to those described above using *Nalp3*$^{-/-}$, *Asc*$^{-/-}$, and *Casp1*$^{-/-}$ macrophages. M-CSF-derived BM macrophages from WT and inflammasome-deficient mice were used in this experiment. As shown in Figure 3A, macrophages deficient in NALP3, ASC, or caspase-1 failed to secrete IL-1β in response to silica and alum, which is consistent with previously published reports. However, macrophages from inflammasome-deficient mice produced slightly higher amounts of PGE_2 in response to silica and alum than cells from WT mice. IL-6 production was previously shown to be independent of the NALP3 inflammasome (Kumar et al., 2009; Yamamoto et al., 2004). Indeed, WT and inflammasome-deficient macrophages produced comparable amounts of IL-6. Similar results were obtained when we performed the same experiments with granulocyte-macrophage colony stimulating factor (GM-CSF)-derived macrophages (Figure 3B). These results indicate that silica and alum induce macrophages to produce PGE_2 through NALP3 inflammasome-independent mechanisms.

PGE_2 synthesis is regulated by cyclooxygenase (COX) and PGE synthase. In particular, COX-2 and PTGES (also known as mPGES-1) have been reported to regulate stimulation-dependent PGE_2 production in macrophages (Kuroda and Yamashita, 2003; Uematsu et al., 2002). As shown in Figure 3C, treatment with NS-398, which is a COX-2-specific inhibitor, significantly suppressed PGE_2 production in silica-activated macrophages. Similar to COX-2 inhibition, *Ptges*$^{-/-}$ macrophages did not produce detectable amounts of PGE_2 upon stimulation with silica (Figure 3D). However, neither COX-2 inhibition nor PTGES deficiency had an effect on silica-induced IL-1β production in macrophages, suggesting that IL-1β production and activation of the inflammasome are independent of PGE_2 production (Figure S3). Similar results were obtained when we performed the same experiments with alum-activated macrophages (data not shown). We then assessed the expression of COX-2 and PTGES in macrophages upon stimulation with silica and alum. As shown in Figure 3E, priming of macrophages with LPS induced the expression of the COX-2 and PTGES proteins. However, silica, alum, and ATP stimulation had no effect on COX-2 and PTGES expression in macrophages. This result indicates that silica- and alum-induced PGE_2 production in macrophages does not involve increased expression of COX-2 or PTGES. Collectively, these results indicate that silica- and alum-induced PGE_2 production in macrophages is mediated by the COX-2 and PTGES pathways.

Silica- and Alum-Induced Production of PGE_2 by Macrophages Regulates Immune Responses In Vivo

Given that *Ptges*$^{-/-}$ macrophages cannot produce PGE_2 while retaining inflammasome function and the ability to produce IL-1β in response to silica and alum (Figure 3 and Figure S3), we determined whether alum-induced PGE_2 production plays a role in regulating immune responses in vivo. We immunized *Ptges*$^{+/+}$ and *Ptges*$^{-/-}$ mice with alum plus OVA twice (day 0 and 7). Ten days after the last immunization, sera were collected and analyzed for amounts of OVA-specific IgE, IgG1, and IgG2c antibodies. In *Ptges*$^{+/+}$ mice, OVA-alum immunization stimulated the generation of OVA-specific IgE, IgG1, and IgG2c. In contrast, *Ptges*$^{-/-}$ mice displayed reduced amounts of OVA-specific IgE (Figure 4A). In contrast, the amounts of IgG1 and IgG2c in the sera taken from *Ptges*$^{+/+}$ and *Ptges*$^{-/-}$ mice were comparable (Figure 4A).

Because previous reports have shown that OVA-silica immunization induces OVA-specific antibody responses (Kumar et al., 2009), we assessed whether silica could trigger IgE responses. As shown in Figure 4B, OVA-silica immunization induced the generation of OVA-specific IgE, IgG1, and IgG2c antibodies. As observed with OVA-alum immunization, OVA-silica-immunized *Ptges*$^{-/-}$ mice displayed reduced amounts of OVA-specific IgE. In contrast, amounts of OVA-IgG1 and IgG2c antibodies were comparable between *Ptges*$^{+/+}$ and

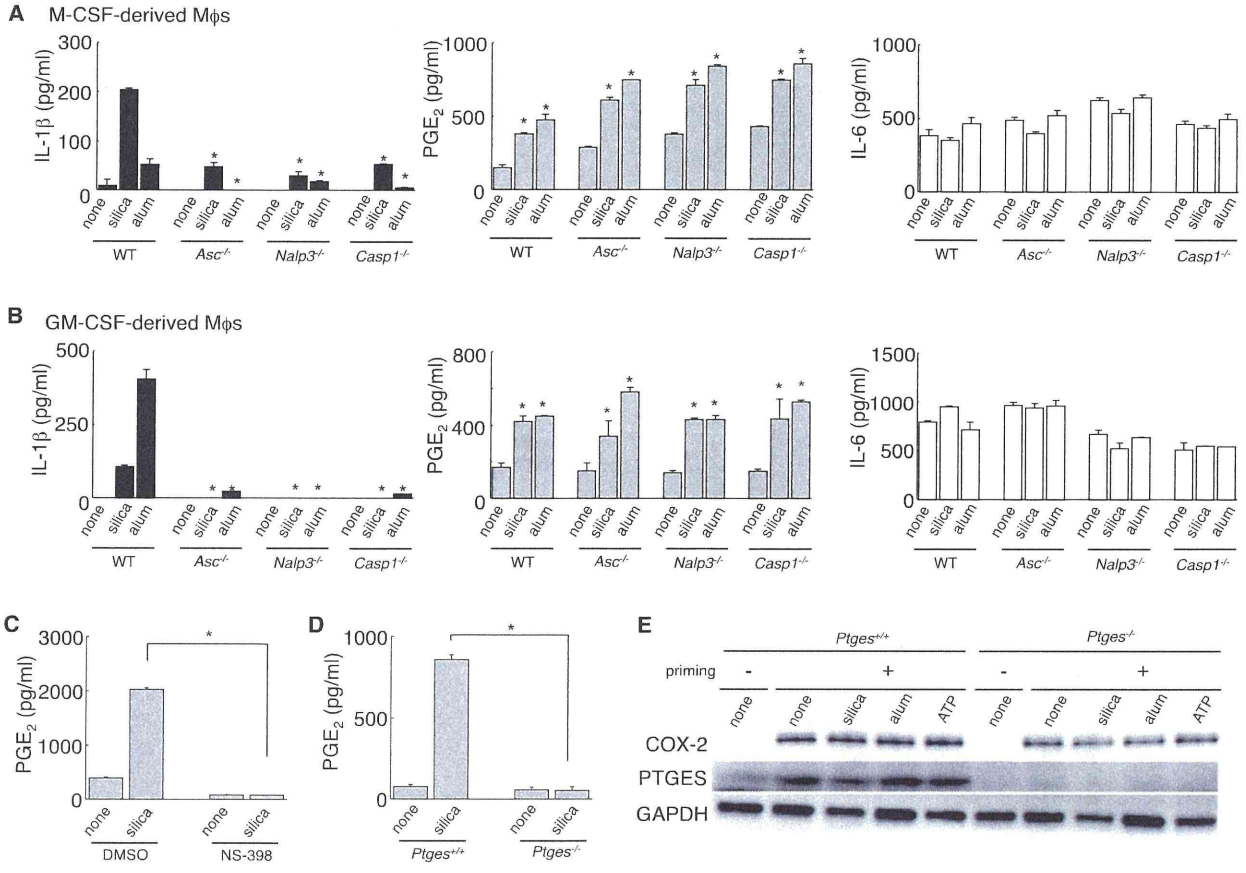

Figure 3. The Mechanisms of Particulate-Induced PGE_2 Production

(A and B) Silica- and alum-induced PGE_2 production is independent of the NALP3 inflammasome. M-CSF- (A) or GM-CSF- (B) derived BM macrophages from WT (C57BL/6), *Asc*$^{-/-}$, *Nalp3*$^{-/-}$, and *Casp1*$^{-/-}$ mice were primed with low-dose LPS and then stimulated with 100 μg/ml silica or 400 μg/ml alum for 6 hr.

(C–E) Silica-induced PGE_2 production is mediated by COX-2 and PTGES.

(C) LPS-primed BALB/c peritoneal macrophages were stimulated with 100 μg/ml silica in the presence or absence of the COX-2 inhibitor NS-398 for 2 hr.

(D) Peritoneal macrophages from *Ptges*$^{+/+}$ and *Ptges*$^{-/-}$ mice were primed with low-dose LPS and then stimulated with 100 μg/ml silica for 2 hr.

(E) *Ptges*$^{+/+}$ and *Ptges*$^{-/-}$ macrophages were primed with or without LPS and stimulated with 100 μg/ml silica, 400 μg/ml alum, or 1 mM ATP for 2 hr. Cell lysates were analyzed for COX-2, PTGES, and GAPDH (loading control) expression by western blotting. Data represent mean ± SE of two (A and B) or three (C and D) independent experiments (*$p < 0.01$).

Ptges$^{-/-}$ mice. We carried out similar in vivo experiments using *Nalp3*$^{-/-}$ and *Casp1*$^{-/-}$ mice, and we found that the amounts of OVA-IgE from WT and mutant mice were comparable (Figure S4A). We also assessed the effect of a Th1 cell adjuvant, *Propionibacterium* (*P.*) *acnes*, on antigen-specific IgE, IgG1, and IgG2c production in vivo. We found that *P. acnes* induced comparable amounts of OVA-IgG1 and IgG2c in *Ptges*$^{+/+}$ and *Ptges*$^{-/-}$ mice and did not induce OVA-IgE in either genotype (Figure S4B). Although *Ptges*$^{-/-}$ mice displayed reduced amounts of OVA-IgE after immunization, the total IgE concentrations were similar in unimmunized *Ptges*$^{+/+}$ and *Ptges*$^{-/-}$ mice (Figure S4C). This result indicates that *Ptges*$^{-/-}$ mice, unlike *Il4*$^{-/-}$ or *Stat6*$^{-/-}$ mice, are not Th2 cell type prone.

We also immunized hematopoietic PGD synthase-deficient (*Ptgds*$^{-/-}$) mice, in which macrophages cannot produce PGD_2, with OVA-alum and analyzed sera for amounts of OVA-specific IgE. As shown in Figure 4C, the amounts of OVA-specific IgE in the sera were similar in WT and *Ptgds*$^{-/-}$ mice. These results indicate that silica- and alum-induced PGE_2 production contributes to the generation of IgE antibodies in vivo. In fact, we found that PGE_2 promoted the production of IgE in spleen cells stimulated with LPS plus IL-4 or anti-CD40 plus IL-4 in vitro (Figure S4D).

Mice that received OVA alone did not exhibit an increase in OVA-specific serum IgE levels and, in fact, exhibited 50-fold lower amounts of OVA-specific IgG1 and IgG2c (Figure 5C and data not shown).

Particulate Nickel Oxide Induces Macrophages to Produce PGE_2, but Not IL-1β, and Enhances IgE production In Vivo

Nickel oxide (NiO) could induce macrophages to produce PGE_2, but not IL-1β or IL-18. NiO is a nanoparticle known to cause lung inflammation when inhaled (Nishi et al., 2009; Ogami et al., 2009). To determine whether NiO could activate macrophages, we

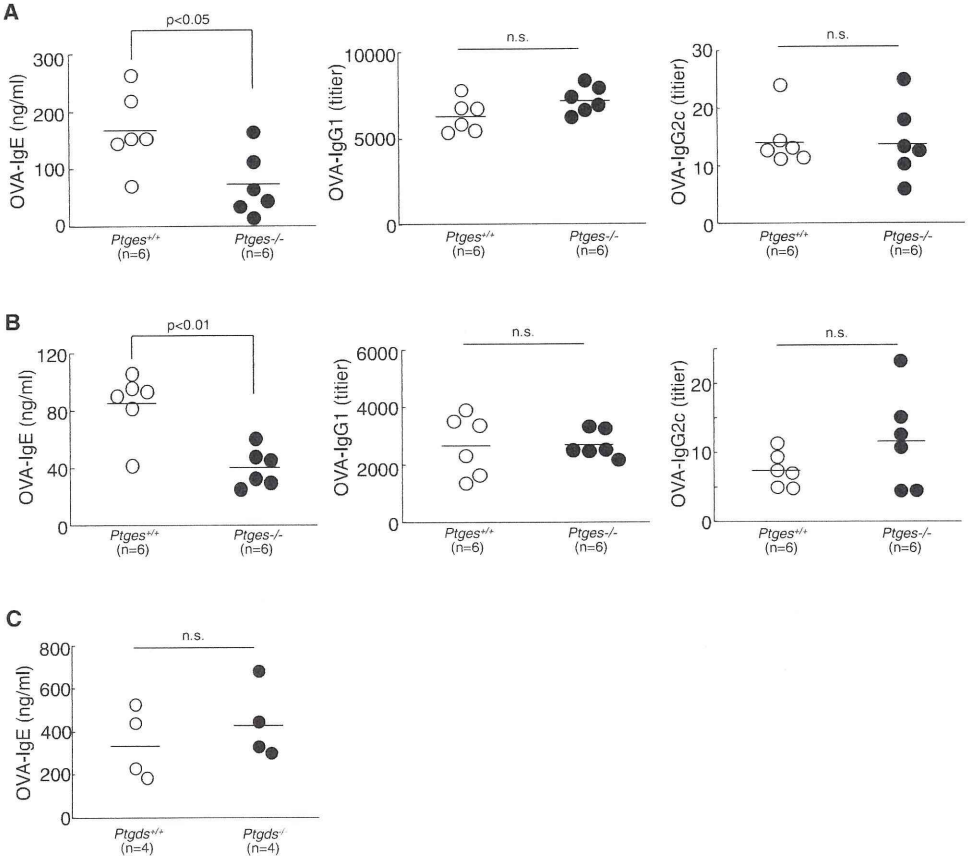

Figure 4. *Ptges*$^{-/-}$ Mice Display Reduced Antigen-Specific IgE Levels after Immunization with Silica or Alum

(A and B) *Ptges*$^{+/+}$ and *Ptges*$^{-/-}$ mice (n = 6) were immunized twice (day 0 and 7) with OVA plus alum (A) or OVA plus silica (B). Ten days after the last immunization, sera were collected and analyzed for OVA-specific IgE, IgG1 and IgG2c antibodies by ELISA.

(C) *Ptgds*$^{+/+}$ and *Ptgds*$^{-/-}$ mice (n = 4) were immunized twice (day 0 and 7) with OVA plus alum. Ten days after the last immunization, sera were collected and analyzed for OVA-specific IgE antibodies by ELISA.

carried out experiments similar to those in which we used silica and alum. We found that, as observed with TiO_2 (Figure 1D), NiO failed to induce IL-1β production in LPS-primed macrophages (Figure 5A). However, NiO-activated macrophages produced significant amounts of PGE_2 at amounts comparable to silica-activated macrophages. As expected, NiO-induced PGE_2 production in macrophages is independent of the NALP3 inflammasome (Figure 5B). In addition, mice immunized with OVA plus NiO exhibited a significant increase in OVA-specific serum IgE concentrations (Figure 5C). In contrast, TiO_2, which did not activate the NALP3 inflammasome or induce PGE_2 production in macrophages in vitro (Figures 1D and 5A), stimulated much weaker IgE responses than immunization with alum and NiO (Figure 5C). These results indicate that particulates that induce PGE_2 production, but not inflammasome activation in macrophages, positively regulate the generation of IgE antibodies in vivo.

Silica-Dependent PGE_2 Production Is Regulated by the Syk and the p38 MAP Kinase Pathway

The mechanisms through which silica, alum, and ATP induce the production of PGE_2 in macrophages are unclear. Therefore, we sought to determine which signaling pathway was involved in the production of PGE_2. To this end, we stimulated LPS-treated macrophages with silica in the presence or absence of various signaling inhibitors, and we then determined which inhibitor(s) suppressed PGE_2 but had no effect on the production of IL-1β. As shown in Figure 6A, only wortmannin suppressed silica-induced production of IL-1β. In contrast, SB203580, U0126, and SP600125 suppressed silica-induced production of PGE_2. We also found that cyclosporin A, rapamycin, and wedelolactone partially suppressed silica-induced PGE_2 production. We conducted similar experiments by using ATP-activated macrophages. SB203580 and wortmannin enhanced ATP-induced IL-1β production, whereas the other inhibitors reduced IL-1β production. With the exception of rapamycin, all the inhibitors reduced PGE_2 production in ATP-activated macrophages (Figure 6B). It is worth noting that SB203580 had no effect on the amounts of COX-2 and PTGES expressed by macrophages (Figure S5A). Taken together, these data suggest that the p38 MAP kinase inhibitor SB203580 preferentially suppresses the production of PGE_2 in both silica- and ATP-activated macrophages. We also sought to ascertain whether silica and ATP

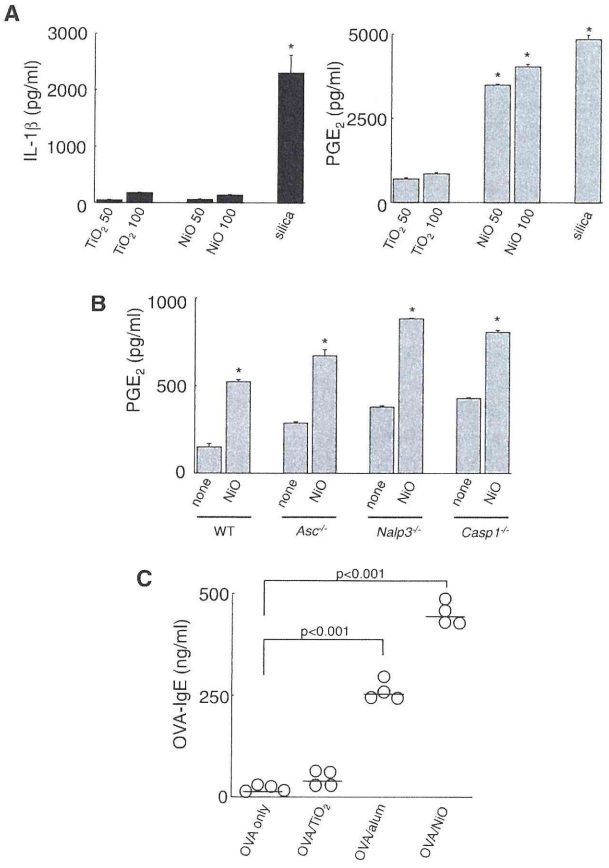

Figure 5. NiO Functions as a Th2 Adjuvant

(A) LPS-primed BALB/c peritoneal macrophages were stimulated with 100 μg/ml silica, 50 or 100 μg/ml NiO, or 50 or 100 μg/ml TiO_2 for 2 hr.

(B) BM-derived macrophages from WT (C57BL/6), *Asc*$^{-/-}$, *Nalp3*$^{-/-}$ or *Casp1*$^{-/-}$ mice were primed with low-dose LPS and then stimulated with 100 μg/ml NiO for 6 hr. Data represent mean ± SE of two (B) or three (A) independent experiments (*$p < 0.01$).

(C) C57BL/6 mice (n = 4) were immunized twice (day 0 and 7) with OVA alone, OVA plus TiO_2, OVA plus alum, or OVA plus NiO. Ten days after the last immunization, sera were collected and analyzed for OVA-specific IgE antibodies by ELISA.

could activate p38 MAP kinase in macrophages and found that stimulation of LPS-primed macrophages with silica and ATP induced p38 MAP kinase phosphorylation and activation (Figure 6C). Several reports have shown that ATP stimulates p38 MAP kinase, which then activates cytosolic phospholipase A_2 ($cPLA_2$) (Gijón et al., 2000; Ulmann et al., 2010). As shown in Figure 6D, treatment with a $cPLA_2$ inhibitor preferentially suppressed PGE_2 production, but not IL-1β production (data not shown), in both ATP- and silica-activated macrophages.

Next, we examined the mechanisms involved in silica-mediated activation of p38 MAP kinase. We have shown that lysosomal rupture by Leu-Leu-OMe activated macrophages to produce PGE_2 (Figure 2E). However, SB203580 significantly suppressed the production of PGE_2 but not IL-1β in Leu-Leu-OMe-treated macrophages (Figure 6E). In addition, treatment of macrophages with poly-2-vinylpyridine-N-oxide (PVNO), which is a lysosomal stabilizing agent (Allison et al., 1966; Von Behren et al., 1983), also suppressed silica-induced PGE_2 production, which was similar to SB203580 treatment (Figure 6F). Treatment with PVNO had no effect on ATP-induced PGE_2 production, given that ATP is not involved in lysosome damage (Hornung et al., 2008). These results indicate that lysosomal damage is involved in PGE_2 production via the activation of p38 MAP kinase in silica-activated macrophages.

Several reports indicate that Syk plays an important role in antifungal responses by activating the NALP3 inflammasome (Gross et al., 2009). In addition, Syk has been shown to be involved in malarial hemozoin-mediated and monosodium urate crystal-mediated inflammasome activation (Ng et al., 2008; Shio et al., 2009). A Syk inhibitor markedly suppressed the production of PGE_2 in both silica- and Leu-Leu-OMe-treated macrophages (Figure 6G). In contrast, Syk inhibition partially suppressed ATP-induced PGE_2 production, suggesting that the signaling pathway involved in PGE_2 production is different between particulate- and ATP-activated macrophages. Syk was partially associated with IL-1β production in silica-stimulated macrophages (Figure 6G). In addition, knockdown of Syk by siRNA in macrophages significantly reduced PGE_2 and IL-1β production compared to cells transfected with control siRNA (Figures S5B and S5C). Syk might act upstream of p38 MAP kinase because Syk inhibition suppressed phosphorylation of p38 MAP kinase in silica-stimulated macrophages (Figure 6H). Taken together, these results suggest that lysosomal damage triggers Syk activation, and then activated Syk upregulates $cPLA_2$ activity via the phosphorylation of p38 MAP kinase.

DISCUSSION

The NALP3 inflammasome has been reported to be activated by alum and involved in alum adjuvanticity and IgE production (Eisenbarth et al., 2008; Kool et al., 2008; Li et al., 2008). However, whether the NALP3 inflammasome is required for alum adjuvanticity is controversial. Here, we found that silica, alum, and ATP, which normally activate the NALP3 inflammasome, stimulate macrophages to produce PGE_2 through mechanisms that do not involve the NALP3 inflammasome. We also found that PGE_2 production by macrophages regulates the generation of antigen-specific IgE antibody in vivo.

The cells of the innate immune system can sense cellular danger and stress via the NALP3 inflammasome. Particulates, such as silica and alum, function as danger signals to activate the NALP3 inflammasome. We found that lysosomal damage and rupture and the subsequent leakage of lysosomal enzymes into the cytoplasm promoted the production of PGE_2 by macrophages. These results demonstrate that the danger signal caused by particulate-induced phagosomal destabilization activates the NALP3 inflammasome and induces macrophages to produce PGE_2. However, *Nalp3*$^{-/-}$, *Asc*$^{-/-}$, and *Casp1*$^{-/-}$ macrophages produced PGE_2 in amounts similar to WT macrophages, suggesting that the lysosomal damage caused by silica and alum activates at least two different pathways, the NALP3 inflammasome pathway and the PGE_2-inducing pathway. We also examined the pathway involved in PGE_2 induction and found that lysosomal damage triggered the production of PGE_2 via the

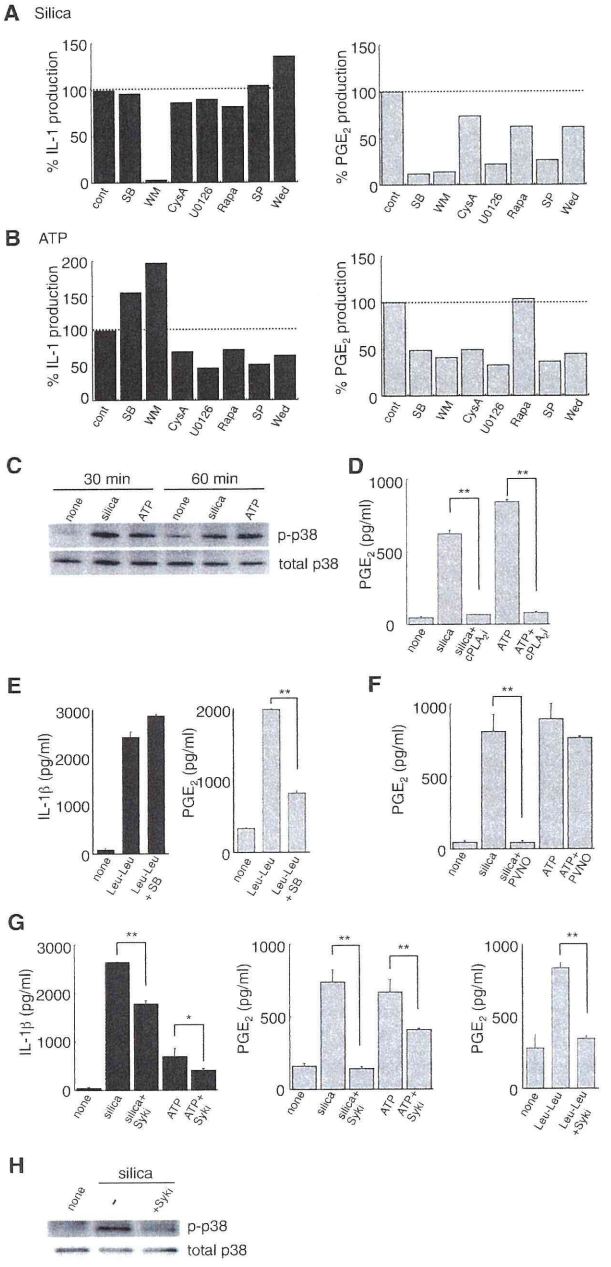

Figure 6. Silica-Induced PGE_2 Production in Macrophages Is Regulated by the Syk/p38 MAP Kinase Pathway

(A and B) LPS-primed BALB/c peritoneal macrophages were stimulated with 100 μg/ml silica (A) or 1 mM ATP (B) for 2 hr in the presence or absence of signaling inhibitors as described in the Experimental Procedures. The results are expressed as the percentage (%) of IL-1β and PGE_2 produced, and the amounts of IL-1β and PGE_2 produced by macrophages stimulated with silica or ATP in the absence of inhibitors were used as the 100% controls.

(C) Macrophages were stimulated with 100 μg/ml silica or 1 mM ATP for the indicated time. Cell lysates were subjected to western blot analysis with anti-phospho-p38 MAP kinase and total p38 MAP kinase antibodies.

(D) LPS-primed macrophages were stimulated with silica or ATP for 2 hr in the presence or absence of 10 μM $cPLA_2$ inhibitor (cPLAi).

(E) LPS-primed macrophages were incubated with 1 mM Leu-Leu-OMe for 2 hr in the presence or absence of p38 MAP kinase inhibitor.

(F) Macrophages were incubated with or without 20 μg/ml PVNO for 5 hr. Then cells were primed with LPS. Primed macrophages were stimulated with silica or ATP for 2 hr.

(G) LPS-primed macrophages were stimulated with 100 μg/ml silica, 1 mM ATP, or 1 mM Leu-Leu-OMe for 2 hr in the presence or absence of 1 μM Syk inhibitor (Syki).

(H) Macrophages were stimulated with 100 μg/ml silica for 30 min in the presence or absence of 1 μM Syk inhibitor. Cell lysates from stimulated macrophages were subjected to western blot analysis. Data represent mean ± SE of two (C and H) or three (A, B, and D–G) independent experiments (*$p < 0.05$, **$p < 0.01$).

activation of Syk and the p38 MAP kinase. Syk is known to play an important role in adaptive immune receptor signaling (Mócsai et al., 2010), and it is involved in malarial hemozoin-mediated and monosodium urate crystal-mediated inflammasome activation (Ng et al., 2008; Shio et al., 2009). Monosodium urate crystals have been reported to induce prostaglandin synthesis in phagocytic cells (Gordon et al., 1985), and we also found that monosodium urate crystals stimulates macrophages to produce PGE_2 and IL-1β in our experimental system (data not shown). In addition, $cPLA_2$ activation and prostaglandin production are regulated by the activation of Syk (Suram et al., 2006). We also found that curdlan, which activates Dectin-1 and Syk, stimulated macrophages to produce higher amounts of PGE_2 in a Syk- and p38 MAP kinase-dependent manner (data not shown). Thus, Syk activation triggered by lysosomal damage promotes the production of PGE_2 in macrophages.

We demonstrated that the p38 MAP kinase pathway is critical for PGE_2 (but not IL-1β) production in silica- and ATP-stimulated macrophages. Several reports have shown that p38 MAP kinase activates $cPLA_2$ and induces arachidonic acid release and PGE_2 secretion in a similar manner as Syk (Gijón et al., 2000; Ulmann et al., 2010). In addition, Syk has been reported to be required for p38 MAP kinase activation under the stress conditions (He et al., 2002). We showed that Syk inhibition suppressed phosphorylation of the p38 MAP kinase. These reports and our findings suggest that Syk activates $cPLA_2$ and PGE_2 production via the p38 MAP kinase pathway in particulate-activated macrophages.

We also found that ATP stimulated macrophages to induce PGE_2 production. However, the required signaling pathway might be different between particulate- and ATP-activated macrophages. Inhibition of the p38 MAP kinase and $cPLA_2$ significantly suppressed PGE_2 production in both silica- and ATP-activated macrophages. In contrast, Syk inhibition partially suppressed ATP-induced PGE_2 production. We have shown that lysosomal damage triggers Syk activation, and ATP has been reported to not be involved in lysosome damage (Hornung et al., 2008). However, ATP stimulation regulates Syk in osteoclasts (Hazama et al., 2009). Hazama et al. and our findings suggest that ATP-activated Syk is partially involved in PGE_2 production in macrophages independent of lysosomal damage. The detailed mechanism involved in lysosomal damage-triggered activation of Syk and p38 MAP kinase remains unclear. In addition, the involvement of cathepsin B in PGE_2 production should be clarified. As such, we are currently investigating which